

2021-11-15

# Metal pollutant pathways in cohesive coastal catchments: Influence of flocculation and biopolymers on partitioning and flux

Schindler, Robert

<http://hdl.handle.net/10026.1/17431>

---

10.1016/j.scitotenv.2021.148800

Science of the Total Environment

Elsevier

---

*All content in PEARL is protected by copyright law. Author manuscripts are made available in accordance with publisher policies. Please cite only the published version using the details provided on the item record or document. In the absence of an open licence (e.g. Creative Commons), permissions for further reuse of content should be sought from the publisher or author.*

2 AVAILABLRE AT:

3 Science of The Total Environment 795:148800-148800 Article number 148800 Nov 2021

4 Metal pollutant pathways in cohesive coastal catchments: Influence of  
5 Flocculation and Biopolymers on Partitioning and Flux.

6 Authors: Schindler, R.J.<sup>1</sup>, Comber, S.D.W.<sup>1\*</sup> and Manning, A.J.<sup>2,3</sup>

7 Affiliations:

8 1. School of Geography, Earth & Environmental Science, Plymouth University, UK.

9 2. School of Biological and Marine Sciences, Plymouth University, UK.

10 3. HR Wallingford Ltd, Howbery Park, Wallingford, UK.

11 \*Corresponding author: sean.comber@plymouth.ac.uk

12 ABSTRACT

13 The impacts of the partitioning of potentially toxic metals (PTM) within the estuarine  
14 environment is highly complex, but is of key significance owing to increases in populations  
15 living within such sensitive environments. Although empirical data exist for the partitioning of  
16 metals between the dissolved and particulate phases, little is known regarding the impacts of  
17 extracellular polymeric substances (EPS) upon the flocculation of particles within such a  
18 dynamic system nor the resultant influence on the distribution of metals between the particulate  
19 and dissolved phases. This prevents regulators from fully understanding the fate and risks  
20 associated with metals in estuaries. This study provides data associated with the simulation of  
21 3 settlings typical of the turbulent mixing found in estuaries and partitioning of copper,  
22 cadmium, nickel, arsenic, lead and zinc for 3 salinities (0, 15, 30 PSU) reflecting the full  
23 salinity range from freshwater to seawater. Experiments were completed with and without the

presence of EPS, using kaolin as the mineral particulate. The results showed significant differences between salinity, PTMs and turbulence for the experiments with and without EPS present. Overall, salinity was the main factor controlling the PTM partitioning to sediment, however the flocculation process did impact on the PTM distribution and with the addition of EPS the impact was more pronounced. The data highlighted the importance of taking account of EPS within any estuarine sediment process modelling, for relying on simple partitioning with corrections for salinity would likely lead to significant bias.

**Keywords:** Potentially Toxic Metals; Partitioning; Flocculation; EPS; Salinity.

## 1. INTRODUCTION

The dispersion of potentially toxic metals (PTMs) into the aquatic environment poses a range of environmental problems. PTMs are released from land-based sources: current and historical mining and smelting industries, industrial and sewage effluents, landfill leachate as well as common use of animal feeds, fertilizers and pesticides, surface runoffs and atmospheric deposition (Taylor & Hudson-Edwards, 2008). They do not degrade, but can change form (speciation) and/or move between the dissolved and particulate phases (partitioning). Global concentrations of PTMs in coastal sediments have increased over 1985–2000 and can affect the ecological balance of freshwater and marine environments for hundreds of years after initial contamination.

Globally, large human populations are concentrated in the narrow zone adjacent to the coast. Lowland rivers and estuaries provide a multitude of ecosystem services such as drinking freshwater supply, fisheries, climate regulation, sheltered access to coastal water, coastal protection, water purification and waste treatment (Millennium Ecosystem Assessment, 2005). Estuaries also serve as nursery areas for many species, provide habitat to a high diversity of sensitive organisms for the whole or part of their life cycle, and are characterized by a high biological productivity. However, estuaries have also been used for the dilution and disposal of waste worldwide (Spencer et al., 2006) which contributes to their deterioration. Bio-assimilation and bio-accumulation of PTMs in aquatic organisms can reach pathogenic and even lethal levels, endangering entire eco-systems and human health (Matta et al., 1999; Hudson-Edwards et al., 1999). Danger to human health is particularly pronounced in the developing world due to poor environmental regulation and a dependency on local water and aquatic food (Luoma & Rainbow, 2008).

PTMs are transported as (1) **particulates** bound to sediments and 2) **solutes** in groundwater and open channel flow. This distinction is an important consideration with respect to their transportation, bioavailability and ultimate environmental fate (Comber et al., 1995). Reactions in which PTMs are reversibly bound to the surface of the sediment matrix are referred to as sorption processes. PTMs desorbed to the water column remain unconstrained and exhibit much great mobility, bioavailability and hence toxicity. Measures to control or minimise dispersion of particles will also control the environmental distribution of PTMs in their particulate phase. In terms of grain-size, the highest metal concentrations are often found in the finest-grained (such as silt- and clay-rich) sedimentary deposits because of the positive relationship between grain surface area (and therefore increased adsorption sites) and metal concentration or as a result of opposite electrical charge, in the case of cationic metals (Zwolsman et al., 1993). Consequently, the particulate-borne phase dominates the transport of PTMs (up to 90% of load, Miller et al., 2007) from land-based sources to the coastal zone (Benoit et al., 1994) and leads to gradual dispersion and accumulation (Dennis *et al.*, 2003).

Prediction and management of PTMs transported from terrestrial sources to the ocean is dependent on an accurate understanding of partitioning between soluble and particulate phases at different spatial and temporal locations within a catchment. PTMs in bed and bank sediments are not permanently fixed but can be periodically remobilized, desorbed, or redistributed between the river to the sea via an estuary (Singh et al., 2005). The ambient conditions that affect partitioning within fluvial and lacustrine environments (e.g., pH, suspended particulate matter concentration (SPM), redox conditions, association with organic carbon and colloidal material) become more complex across the river to sea gradient. Estuarine waters are characterized by strong tidally-driven physicochemical gradients in e.g. salinity, water density, flow velocity and turbulence regimes, and suspended matter composition (Elliott and McLusky, 2002), which are important influences on the fate of metals. These factors lead

to the observed non-conservative behaviour for the majority of metal elements within estuaries (Machado et al., 2016). Notably, estuaries experience saline intrusion resulting in chloro-complexation and formation of insoluble salts with a counter-ion, most commonly sulphide (Comber et al., 1996; Wells, 2019). Furthermore, contamination is expected to increase as more sediments are mobilized with rising sea level and increasing storm frequency (DEFRA, 2014).

The sedimentary make up of most estuaries is dominated by fine-grained mud (silt and clay) (Healey et al., 2002), which is key to the life cycle of indigenous sediment-dwelling organisms (Black et al., 2002) and which influence the chemical nature of the substratum (Meadows et al., 2012). What is less recognised with respect to the sorption, sedimentation and sediment accumulation cycle is the role of flocculation. Flocculation is a dynamically active process dependent on the electrostatic charging of the mineral, and which readily reacts to changes in hydrodynamics, SPM concentration, salinity, organic content and mineralogy. Particles aggregate through collisions to form ‘flocs’, comprising up to  $\sim 10^6$  constituent particles (Manning, 2004). Changes in turbulent shear stress ( $\tau$ ) may both promote floc aggregation and disaggregation (Manning et al., 2017) and, together with salinity, can impose a maximum floc size restriction on suspended sediments that vary spatially and temporally in response to tidal cycles. As flocs grow in size their effective densities generally decrease (Klimpel & Hogg, 1986) and their settling velocities rise due to a Stokes’ Law relationship (Manning & Dyer, 1999). Typically, floc settling velocities are significantly quicker than for individual cohesive particles ( $\sim 1\text{-}5\text{ }\mu\text{m}$  in diameter).

There is an increasing awareness that naturally occurring extracellular polymeric substances (EPS), secreted by bacteria and microphytobenthos (principally diatoms) mediate sediment dynamics in cohesive environments (Spears et al., 2007; Malarkey et al., 2015). EPS occurs at mg/kg levels in sediments and like metals, will partition into the dissolved phase, where

Morelle et al., (2017) have reported soluble concentrations in the mg/l range driven by phytoplankton excretion and microbenthos contributions; thus supporting their role in influencing the flocculation dynamics (Hanlon et al., 2006).

Recent studies show that EPS binds particles together because molecules adhere to particle surfaces, form elastic ‘bridges’ linking grains, fill void space and ultimately envelope grains (Parsons et al., 2016). Once present, EPS is involved in cycles of sediment erosion, transport, flocculation and deposition, exerting a significant influence on sediment dynamics (e.g. Malarkey et al., 2015; Parsons et al., 2016). EPS therefore has the capacity to modulate flocculation by influencing the binding potential of particles within each floc. Moreover, the solubilisation and remineralization due to microbial activity could also affect the stability of flocs (Kjørboe, 2001), via impacting floc size and settling velocity resulting in a more complex sediment dynamics compared with pure-mineral dynamics (Lai et al., 2018).

The determination of particulate-borne PTM load is dependent on the accuracy of partitioning coefficients for individual PTMs. However, significant gaps in our understanding exist in cohesive estuarine environments where flocculation dictates SPM transport and deposition. Knowledge of the association of PTMs with flocculated sediments is limited to a single study in coastal waters (Koron et al., 2013). It is clear that the partitioning of PTMs between soluble and particulate phases, and the flux of associated pollutants, are spatially and temporally variable in response to changing floc characteristics within a tidal catchment. Further, the role of EPS, ubiquitous in estuarine muds, in both the modulation of flocculation dynamics and PTM partitioning is yet to be determined and so forms the focus of this study. It is hypothesized that floc size and settling velocity of the SPM population directly influence key aspects of the SPM-metal sorption:desorption processes via:

- 1) the residency time of remobilized sediments in the water column,

- 2) the surface area of SPM available for sorption exchange
- 3) the cycle of floc aggregation-disaggregation under changing salinity and turbulent shear stresses over tidal times-scales promotes sorption-desorption exchanges
- 4) the ubiquitous presence of EPS may modulate floc characteristics, and consequently sorption processes within an estuary
- 5) EPS may also directly influence partitioning by blocking sorption sites within the floc matrix
- 6) EPS may impact on partitioning through complexation of metal ions with known affinities for organic ligands such as copper and to a lesser extent zinc and nickel.

In addition, the amount of PTMs deposited in the particulate phase will change in response to the mass settling flux (MSF) of sediments - the mass of sediment deposited over an area over time – which is a function of spatial and temporal changes of the flocculated SPM population. These experiments quantify, for the first time, the partitioning coefficients of PTMs in flocculated SPM populations in estuaries. The study also comprises the first controlled assessment of EPS modulation of flocculation dynamics and, by extension, PTM sorption dynamics. By calculating MSF through unique floc measurement techniques, the settling flux of particulate-borne PTMs (PSF) in cohesive estuaries is presented for the first time.

## **2. MATERIALS & METHODS**

The experiments use an annular flume to physically model changing hydrodynamics, salinity and EPS content at (i) **river**, (ii) **estuary** & (iii) **coastal** zones across an idealized mesotidal muddy catchment to quantify:

1. The partitioning coefficients of common PTMs
2. The effects of EPS on partitioning coefficients of common PTMs
3. The effects of EPS on floc characteristics



4. The settling flux of particulate-borne PTMs (PSF)

**Table 1. Salinity and turbulent shear stress combinations of each experiment (repeated with and without EPS addition).**

Salinity	Turbulent Shear Stress, $\tau$
PSU	Pa
<b>0</b>	0.70 = $\tau_{Hi}$
<b>0</b>	0.35 = $\tau_{Int}$
<b>0</b>	0.10 = $\tau_{Low}$
<b>15</b>	0.70 = $\tau_{Hi}$
<b>15</b>	0.35 = $\tau_{Int}$
<b>15</b>	0.10 = $\tau_{Low}$
<b>30</b>	0.70 = $\tau_{Hi}$
<b>30</b>	0.35 = $\tau_{Int}$
<b>30</b>	0.10 = $\tau_{Low}$

## 2.1 Annular Flume & Turbulent Shear Stress

This study utilised a mini-annular flume to create a consistent and repeatable turbulent environment. The annular flume has an outer diameter of 1.2 m, a channel width of 0.1 m and a maximum depth of 0.15 m, with a motor-driven rotating roof to create the flow for cohesive sediment experiments (Manning & Dyer, 1999). Maximum flow speeds of approximately 0.7 m s<sup>-1</sup> can be produced in the lower half of the water column, created by 10 mm deep paddles

attached to the underside of the roof. Three turbulent shear stresses,  $\tau$ , were used to represent variations in hydrodynamic forcing within an estuary (Manning et al., 2009) (Table 1). Each experiment was undertaken twice: Once with a purely mineral suspended particulate matter (*abiotic* case), and repeated with the addition of EPS (*biotic* case).

## **2.2 PTM Additions**

Six potentially toxic metals (PTMs) typical of mining wastes associated with sulphidic ores found in mineral rich locations across the globe were used in each experimental run: arsenic (As), cadmium (Cd), copper (Cu), nickel (Ni), lead (Pb) and zinc (Zn). They are amongst the PTMs considered as Priority Substances, Priority Hazardous Substances and Specific Pollutants by the EU's Water Framework Directive (DEFRA, 2014) and routinely assessed for the UK's Marine Management Organisation marine licence applications.

Spiking concentrations were based on the expected partitioning behaviour of the elements to ensure dissolved concentrations would be measurable after partitioning and dilution. Literature suggests partitioning to the sediment will increase in the order  $\text{Ni} < \text{Cd} < \text{As} < \text{Zn} < \text{Cu} < \text{Pb}$  based on physio-chemical characteristics of the elements themselves as well as their interactions with saline matrices (Comber et al., 1996). Consequently, higher concentrations of lead were spiked into solution compared with nickel as it was expected that lead would partition strongly to the particulates leaving little in the dissolved phase to analyse; whereas nickel would be expected to remain predominantly in solution. The concentration of metal spiked into the flume reflected the partitioning with concentration additions ranging from  $0.1 \text{ mg L}^{-1}$  for Ni to  $2 \text{ mg L}^{-1}$  for lead. The concentration of each PTM in each water sample was determined through ICP-MS post-experiments. For saline runs, samples were diluted by a factor of 5 in order to avoid salt matrix interference in the ICP-MS analysis.

## **2.3 Suspended Particulate Matter**

## *Mineral (Abiotic) Experiments*

The sediment component comprised kaolin clay with a median grain size of 6  $\mu\text{m}$ . The depth-averaged suspended particle matter concentration (SPMC) was maintained at 1.0 g L<sup>-1</sup> for all abiotic experiments. Sediment slurries were prepared using 38.0 g of kaolin in 0.5 L of ultra-pure water.

## *Biotic Experiments*

Xanthan gum, a versatile fine-powdered polysaccharide produced from *Xanthomonas campestris* bacterium, is used as a proxy for EPS. It becomes soluble when added to water and has been previously been used as a proxy for biological cohesion in studies on biomediated sediment transport (e.g., Malarkey et al, 2015; Parsons et al., 2016). EPS concentrations on surface sediments may be up to 5% (dry weight) in intertidal muds (Taylor & Patterson, 1998) and >1% in freshwater muds (Gerbersdorf et al., 2009). Lower concentrations of EPS (0.01–0.1%) have been found pervasively distributed in sandy muds and sands with low mud content (e.g. Patterson et al., 2000). EPS content of the SPM in these experiments was held at 2% - an intermediate value spanning surface deposits (most liable to become suspended) in freshwater and estuarine locations. Kaolin (37.24 g) and EPS (0.76 g) were mixed when dry to ensure homogeneity before the addition of 0.5 L of ultra-pure water to form a slurry.

Gravimetric analysis of extracted water samples were used to ensure the ambient SPMC was within required experimental tolerances across all experiments.

## **2.4 Experimental Procedure**

The capacity of the flume is 38 L and it was filled with 37.5 L of ultra-pure water before the start of each experiment. For saline experiments, salt was progressively added and the flume circulated to mix the salt until the required salinity was reached. The following procedure was followed:

- 1) Metal standards were directly introduced into the water, and mixed through flume circulation for 5 minutes.
  - 2) Trial experiments revealed that the pH of the water after the introduction of metal standards was ~4.5, significantly lower than found in estuaries. A buffer was added to the water to ensure that  $\text{pH} = 8.2 \pm 0.1$ .
  - 3) 3 x 15 ml water samples were taken for Inductively Coupled Plasma-Mass Spectrometry (ICP-MS) analysis to determine the precise initial PTM dissolved concentrations. Samples were diluted 5 fold with ultra-pure water in order to reduce the salt matrix (for 15 and 30 PSU)
  - 4) The sediment slurry (0.5 L) was introduced into the flume and mixed at  $\tau_{Hi}$  for 1 minute, and a second set of water samples taken for ICP analysis.
  - 5) The mixed sediment slurries were sheared in the flume for 30 minutes at  $\tau_{Hi}$ . This duration of shearing was pre-determined in accordance with theoretical flocculation time (van Leussen, 2004).
  - 6) To obtain floc and water samples, the rotation was stopped for approximately 6-8 seconds, although flow in the flume still continued through inertia, maintaining particles in suspension throughout this period (Manning & Whitehouse, 2009). 50 ml samples were extracted using a glass pipette at mid-height of the flow: (1) A sample for floc characterisation, (2) three samples for ICP analysis, and (3) a sample for gravimetric quantification of the SPMC.
  - 7) Steps 5& 6 were repeated at  $\tau_{Int}$  and  $\tau_{Low}$
- The flume was subsequently emptied and cleaned using a high-pressure sprayer and detergents in preparation for the next experiment.

## 2.5 PTM Concentrations of Water Samples

For each experiment, the mean soluble PTM concentrations from initial, sediment-free conditions (see Step 4) were established based on three replicate water samples. Dissolved PTM concentrations were measured. Particulate PTM concentrations were calculated assuming any loss from the dissolved phase was a result of sorption to the particulate matter. A control experiment showed insignificant sorption to the flume apparatus nor loss whilst filtering (2% hydrochloric acid cleaned) 0.4 µm Sartorius cellulose acetate membranes. Subsequently each experiment yielded three mean values concentration in the dissolved phase,  $C_d$ , for each turbulent condition (Step 7):  $a = \tau_{Hi}$ ,  $b = \tau_{Int}$  and  $c = \tau_{Low}$ . The data was used to determine partitioning coefficients,  $K_p$ , which give information on the integrated effects of adsorption and desorption processes:

$$K_p = \frac{C_s}{C_d} \quad [\text{Eq. 1}]$$

where  $C_d$  is the concentration in the dissolved phase ( $\text{mg ml}^{-1}$ ) and  $C_s$  is the concentration of metal in the particulate phase (initial PTM concentration –  $C_d$ ,  $\text{mg g}^{-1}$ ).

## 2.6 Floc Characterisation

Floc sample populations were characterized using LabSFLOC (*‘Laboratory Spectral Flocculation Characteristics’*), a video-based instrument developed at Plymouth University. SPM samples were taken from the water column using a pipette and transferred to the LabSFLOC settling column following protocols outlined in Manning et al., 2017. The SPM was recorded by the video camera as it was settling. The observed flocs were measured within a reference volume of water (0.4 L). Floc size (equivalent spherical diameter,  $D$ ) and settling velocity ( $W_s$ ) were determined for each individual floc directly from video recordings. The effective density ( $\rho_{eff}$ ) of each floc was calculated by applying Stokes’ Law relationship, (Manning et al., 2017):

$$\rho_{eff} = (\rho_f - \rho_w) = \frac{W_s 18 \mu}{D^2 g} \quad [\text{Eq. 2}]$$

where  $\rho_{eff}$  is the difference between the floc bulk density ( $\rho_f$ ) and the water density ( $\rho_w$ ) and  $\mu$  is kinematic viscosity. Mass settling flux,  $MSF$ , is defined as the product of the settling velocity and SPM concentration (Manning, 2004).

### 3. RESULTS AND DISCUSSION

#### 3.1 PTM Sorption and Partitioning

Mean  $K_p$  values with 95% confidence intervals for each PTM in each experiment are shown in Figure 1 & Tables S1 and S2 of the Electronic Supporting Information.  $K_{p(\text{Min})}$  refers to mineral SPM experiments;  $K_{p(\text{Bio})}$  refers to biotic SPM experiments. Large  $K_{p(\text{Min})}$  and  $K_{p(\text{Bio})}$  values under initial  $\tau_{Hi}$  conditions indicate that the majority of physio-chemical processes resulting in adsorption to the floc field occur rapidly (seconds to minutes) (Comber et al., 1996).

There are clear trends in the partitioning of the metals across the varying salinities. For the mineral only phase partition coefficients ( $K_{p(\text{Min})}$ ) clearly decrease with rising salinity across all turbulence shear stresses for As, Cd, Ni, Pb and Zn, with a less distinct trend for Cu (Figure 1 and Table S2). The magnitudes of the partition coefficients are of the same order as reported in the literature and the observed trends driven by a combination of chloro-complexation, electrostatic competition and mass effects (Comber et al., 1995; Heiro et al., 2014; van der Auweraert, 2018). Overall  $K_{p(\text{Min})}$  partition coefficients followed the order Pb>Cu>Zn>Ni>As>Cd from highest to lowest.

The impact of organic chemicals on the partitioning of metals between water and sediment has been explored previously, but mostly by looking at empirical relationships (DeFonseca et al., 2013; Nho et al., 2018).

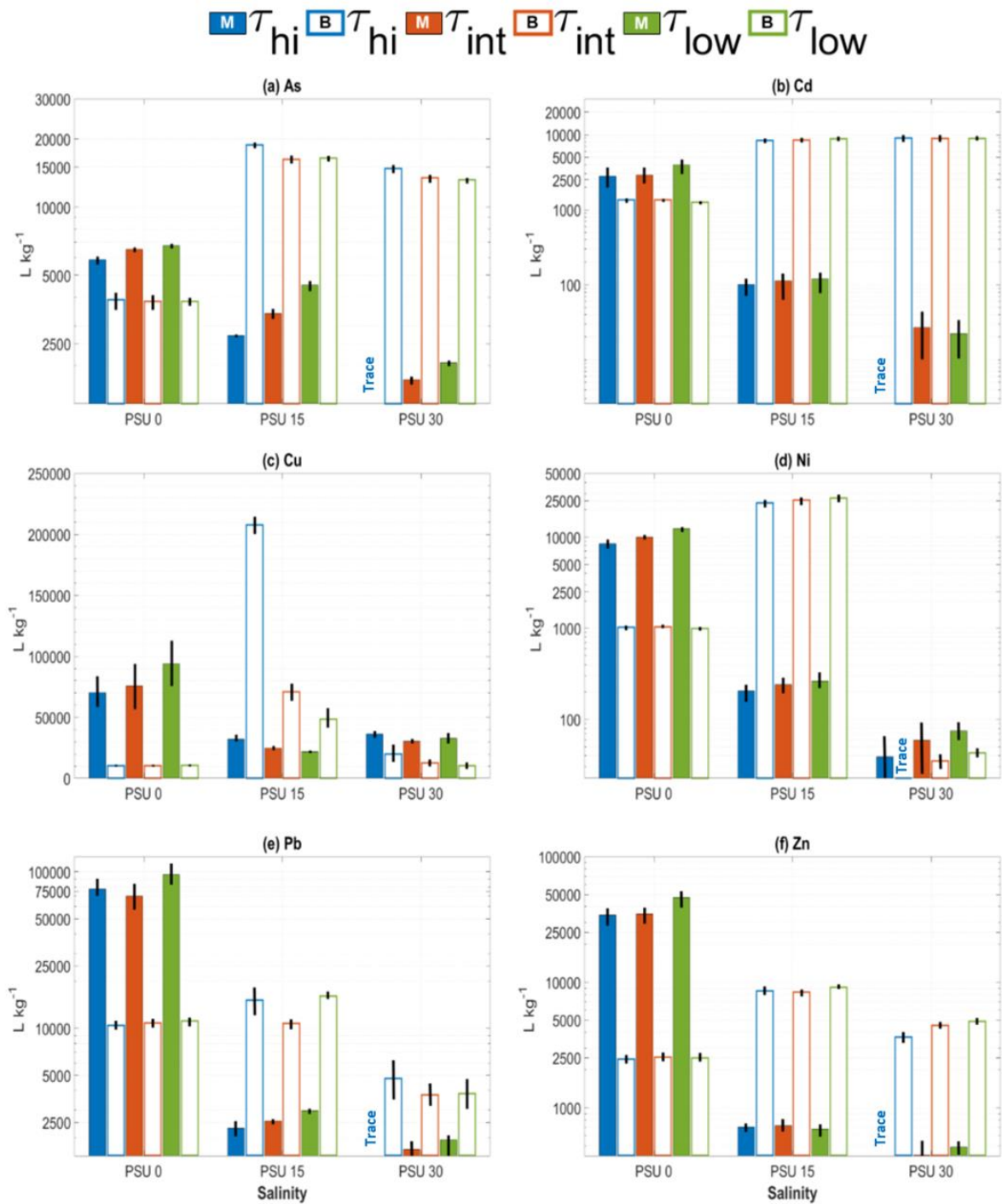


**Figure 1. Partitioning coefficients,  $K_p$ , for each PTM for each experimental run. Solid bars indicate results for mineral SPM; bars with colour outlines indicate results for biotic SPM. Note that all y-axes are logarithmic with the exception of (c) which is linear. Error bars are confidence intervals at 95%.**

However, the partitioning behaviour after the addition of the EPS was considerably different. The magnitude of  $K_{p(\text{Bio})}$  in freshwater (PSU 0, clear bars) show no statistical difference across turbulence regimes for any of the PTMs, but were lower than the equivalent coefficients for the mineral only  $K_{p(\text{min})}$ , for each PTM (reductions in  $K_p$  resulting from the addition of EPS in freshwater are, from largest to smallest:  $\text{Zn} > \text{Ni} > \text{Cu} = \text{Pb} > \text{Cd} > \text{As}$ ; Table 2). This indicates that sorption processes occur in the initial  $\tau_{\text{Hi}}$  conditions, with minimal physio-chemical changes resulting from subsequent reductions in turbulent shear stress. All  $K_{p(\text{Bio})}$  values were lower than  $K_{p(\text{Min})}$  equivalents (Table S1).

For the saline samples  $K_{p(\text{Bio})}$  was, with the exception of lead and nickel, higher than the freshwater samples. For all PTMs other than Cd,  $K_{p(\text{Bio})}$  was lower in the PSU30 samples across all turbulence than the PSU15 case, again largely reflecting the trend of the  $K_{p(\text{Min})}$  dataset. However, other than for Cu and Ni at PSU30, in all cases  $K_{p(\text{Bio})}$  was greater than the equivalent  $K_{p(\text{Min})}$ . Changes in shear stress turbulence impacted on the partitioning of the metals to varying degrees, but generally differences were more subtle than observed with changing the salinity.

For freshwater As, Cu, Ni, Pb and Zn exhibit marginal, but not statistically different increases in  $K_{p(\text{Min})}$  across  $\tau_{\text{Hi}} - \tau_{\text{Low}}$ .  $K_{p(\text{Bio})}$  values for freshwater were effectively identical. At higher salinities, other than for copper at PSU15 where  $K_{p(\text{Bio})}$  decreased across  $\tau_{\text{Hi}} - \tau_{\text{Low}}$  all other PTMs remained consistent (Table S3). For  $K_{p(\text{Min})}$  across  $\tau_{\text{Hi}} - \tau_{\text{Low}}$  significant increases for both PSU15 and PSU30 were observed for As and to a degree Pb and Ni, with no statistical differences for the other PTMs.



309 **Table 2.  $K_{p(\text{Bio})}:K_{p(\text{Min})}$  ratio for each PTM for each turbulence regime and salinity.**

<b>As</b>	<b><math>\tau_{\text{Hi}}</math></b>	<b><math>\tau_{\text{Int}}</math></b>	<b><math>\tau_{\text{Low}}</math></b>	<b>Mean</b>
<b>PSU 0</b>	0.66	0.59	0.57	0.61
<b>PSU 15</b>	6.91	4.78	3.62	5.10
<b>PSU 30</b>	10.9	7.77	6.41	8.36

310

<b>Cd</b>	<b><math>\tau_{\text{Hi}}</math></b>	<b><math>\tau_{\text{Int}}</math></b>	<b><math>\tau_{\text{Low}}</math></b>	<b>Mean</b>
<b>PSU 0</b>	0.48	0.46	0.32	0.42
<b>PSU 15</b>	83.7	75.7	73.8	77.8
<b>PSU 30</b>	3507	331	401	1413

311

<b>Cu</b>	<b><math>\tau_{\text{Hi}}</math></b>	<b><math>\tau_{\text{Int}}</math></b>	<b><math>\tau_{\text{Low}}</math></b>	<b>Mean</b>
<b>PSU 0</b>	0.14	0.14	0.11	0.13
<b>PSU 15</b>	6.50	2.87	2.20	3.86
<b>PSU 30</b>	0.55	0.42	0.28	0.42

312

<b>Ni</b>	<b><math>\tau_{\text{Hi}}</math></b>	<b><math>\tau_{\text{Int}}</math></b>	<b><math>\tau_{\text{Low}}</math></b>	<b>Mean</b>
<b>PSU 0</b>	0.12	0.10	0.08	0.10
<b>PSU 15</b>	116	106	102	108
<b>PSU 30</b>	0.58	0.59	0.57	0.58

313

<b>Pb</b>	<b><math>\tau_{\text{Hi}}</math></b>	<b><math>\tau_{\text{Int}}</math></b>	<b><math>\tau_{\text{Low}}</math></b>	<b>Mean</b>
<b>PSU 0</b>	0.13	0.15	0.12	0.13
<b>PSU 15</b>	6.58	4.19	5.39	5.39

<b>PSU 30</b>	3.14	2.24	1.97	2.45
---------------	------	------	------	------

314

<b>Zn</b>	<b><math>\tau_{Hi}</math></b>	<b><math>\tau_{Int}</math></b>	<b><math>\tau_{Low}</math></b>	<b>Mean</b>
<b>PSU 0</b>	0.07	0.07	0.05	0.07
<b>PSU 15</b>	12.1	11.6	13.4	12.4
<b>PSU 30</b>	8.83	10.8	10.0	9.88

315 The dataset showed that there are considerable differences in adsorption for all PTMs based on  
316 a combination of chemistry (predominantly chloro-complexation) but also contributions from  
317 the interaction between the EPS, inorganic particles and EPS-metal complexation  
318 characteristics. Previous studies have shown the influence of particulate organic matter, of  
319 which EPS would be significant component, to be a controlling factor in the partitioning of  
320 metals in estuaries, but itself will be influenced by salinity (Turner et al., 2004). Furthermore,  
321 colloidal material in estuaries which comprises a mostly poorly defined proportion of organic  
322 and inorganic species also influence the partitioning of PTMs (Wang and Wang, 2016). The  
323 complex interplay between these factors ultimately determines the partitioning characteristics  
324 of the PTMs (Feng et al., 2017).

325 Under freshwater conditions  $K_{p(Min)} > K_{p(Bio)}$  for all PTMs. Conversely, at 15 PSU,  $K_{p(Bio)} >$   
326  $K_{p(Min)}$  for all PTMs resulting from both a reduction in adsorption for mineral SPM and  
327 increases for biotic SPM when compared with freshwater. For most PTMs the reduction in  
328 turbulent shear stress causes adsorption in both mineral and biotic SPM to change in the same  
329 manner, reflecting physical, rather than chemical control mechanisms. However, for As and Pb  
330  $K_{p(Min)}$  values increase while (much larger)  $K_{p(Bio)}$  values decrease.

### 331 **3.2 Flocculation Characteristics**

332 Figure 2 shows the distribution of size versus settling velocity of flocculated particles within  
333 the SPM for each experimental scenario. Figure 3 and Table S4 summarise the mean primary

characteristics of each floc population. Mean floc size for mineral SPM ( $D_{(Min)}$ ), under  $\tau_{Hi}$  increases with salinity, reflecting the improved efficiency of flocculation under increasing electrostatic charging of the sediment. Mean settling velocity ( $W_{s(Min)}$ ), rises 3-fold under high shear stresses, with commensurate reductions in mean effective density ( $\rho_{eff}$ ), following Stokes' Law (Eq. 2) (Manning and Dyer, 1999). The reduced density of the floc population reflects the small increase in mean porosity ( $Por_{(Min)}$ ). The total surface area ( $A_{min}$ ) of a floc population is a function of the floc size, frequency ( $n$ ), and SPM concentration ( $SPMC$ ) and is shown to increase with salinity under  $\tau_{Hi}$  conditions (Figure 3).  $SPMC_{(Min)}$ , however, decreases as a result of higher settling velocities of larger, less dense flocs (Klimpel and Hogg, 1986). Similarly, the floc frequency ( $n_{(Min)}$ ) declines, which is both a function of lower  $SPMC_{(Min)}$  and more efficient flocculation, which results in larger flocs comprised of more primary particles (Manning, 2004). This indicates that surface area is principally controlled by floc size ( $D$ ) rather than floc frequency ( $n$ ) and  $SPMC$ . The mass settling flux ( $MSF$ ) is a function of settling velocity ( $W_s$ ), effective floc density ( $\rho_{eff}$ ) and  $SPMC$ .  $MSF_{(Min)}$  under  $\tau_{Hi}$  conditions increases significantly from 1.9 to 5.3 g m<sup>-2</sup> s<sup>-1</sup> from 0 – 30 PSU, a factor of 2.5, indicating that increases in settling velocity ( $W_{s(Min)}$ ) dominate over reductions in effective density ( $\rho_{eff}$ ) and total particulate matter concentrations ( $SPMC$ ).

Under  $\tau_{Int}$  conditions,  $D_{(Min)}$  rises from 0 – 15 PSU then falls from 15 – 30 PSU, in contrast to the constant increase seen for  $\tau_{Hi}$ .  $D_{(Min)}$  is also lower than under  $\tau_{Hi}$  conditions for each salinity, notably for 30 PSU where  $D_{(Min)}$  is half that of  $\tau_{Hi}$  conditions.  $W_{s(Min)}$  increases with salinity but is also lower than  $\tau_{Hi}$  conditions. Conversely,  $\rho_{eff(Min)}$  is statistically similar for 0 PSU and higher for saline conditions than  $\tau_{Hi}$ , exhibiting a rise and fall around 15 PSU commensurate with changes in  $D_{(Min)}$ . These contrasts with  $\tau_{Hi}$  reflect the lower rate of collision under a reduced turbulent shear stress.

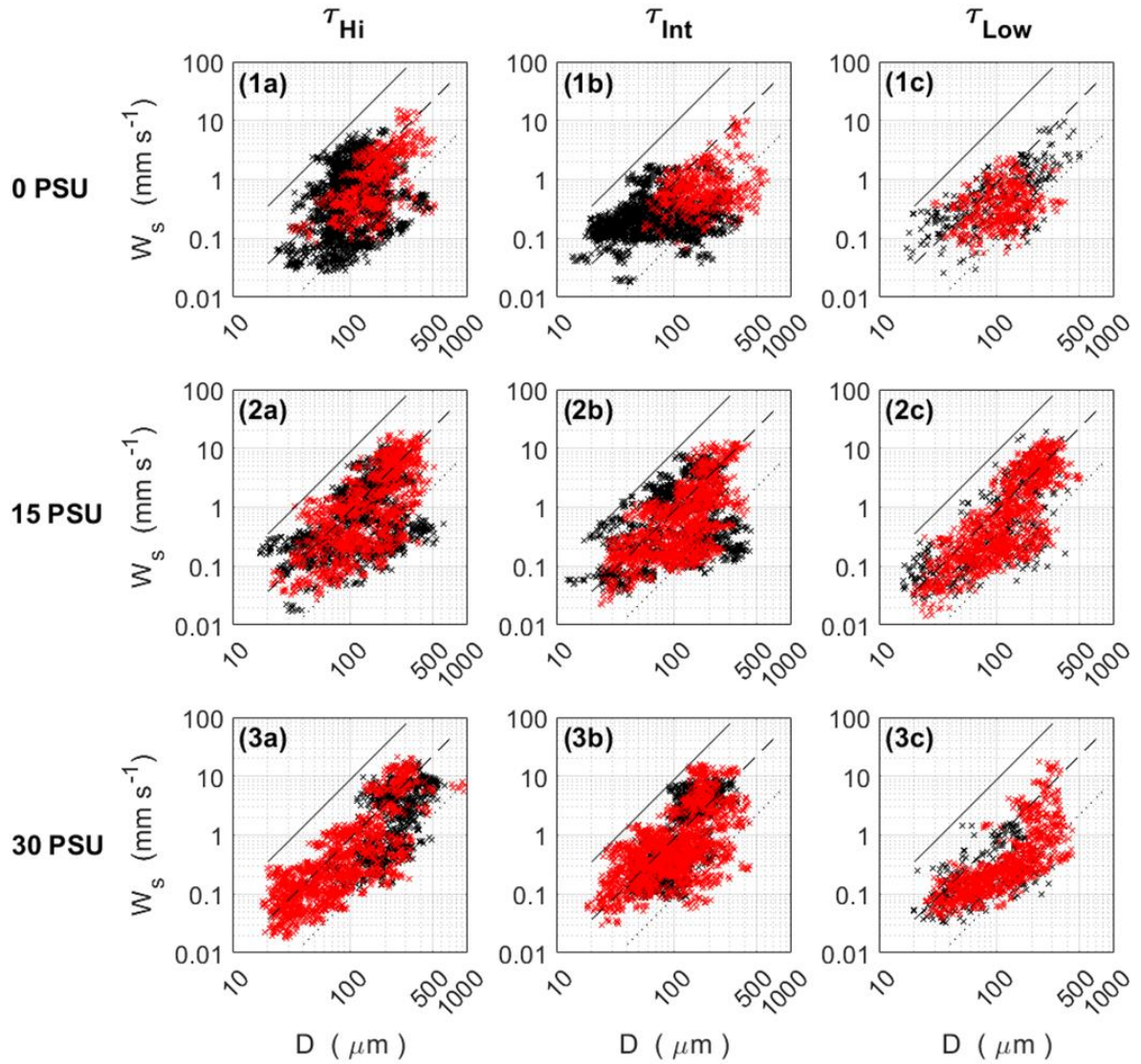


**Figure 2: Relationship between flocculation size,  $D$ , and settling velocity,  $W_s$ , for all experiments. Both axes are logarithmic. Each observation represents a single floc within the SPM population. Black observations are for mineral SPM; red observations are for biotic SPM. Diagonal lines show different values of effective density,  $\rho_{eff}$ , for reference: 1600 ( — ), 160 ( - - - ) and 16 ( ..... )  $\text{kg m}^{-3}$**

369  $A_{(\text{Min})}$  shows a similar rise and fall around 15 PSU, despite an inverse pattern in  $n_{(\text{Min})}$  and  
 370  $SPMC_{(\text{Min})}$ . Compared with  $\tau_{Hi}$  conditions,  $A_{(\text{Min})}$  is lower for  $\tau_{Int}$  to a very similar degree seen  
 371 for  $D_{(\text{Min})}$ , indicating that  $D_{(\text{Min})}$  principally controls surface area (Figure 2).  $SPMC_{(\text{Min})}$  is also  
 372 consistently lower in  $\tau_{Int}$ , despite slower mean settling velocities, which is indicative of the  
 373 reduced turbulent energy available to maintain particles in suspension.  $MSF_{(\text{Min})}$  is reduced as  
 374 a consequence of both lower  $SPMC_{(\text{Min})}$  and  $W_{s(\text{Min})}$ , despite higher mean effective density at  
 375 15 and 30 PSU.

376 Under  $\tau_{Low}$  conditions, the mean floc size ( $D_{(\text{Min})}$ ) is the largest for mineral SPM under  
 377 freshwater conditions. Conversely, under saline conditions  $D_{(\text{Min})}$  values are smaller than other  
 378 turbulence regimes.  $D_{(\text{Min})}$  at 15 PSU is statistically similar but decreases 30 PSU. The mean  
 379 settling velocity ( $W_{(\text{min})}$ ) rises between 0 PSU and 15 PSU and is higher than the equivalent  
 380 under intermediate shear stress conditions, but falls at 30 PSU then falls significantly at 30  
 381 PSU. Floc frequency,  $n_{(\text{Min})}$ , and  $SPMC_{(\text{min})}$  are considerably lower at each salinity than for  
 382 other turbulence regimes. This indicates that turbulent shear stress is insufficient to suspended  
 383 most of the SPM at the measurement height in the water column, despite  $W_{s(\text{Min})}$  values  
 384 comparable with higher turbulence regimes. Consequently,  $A_{(\text{Min})}$  is significantly lower under  
 385  $\tau_{Hi}$  and  $\tau_{Int}$  conditions.  $MSF_{(\text{Min})}$  under 0 PSU is  $0.46 \text{ g m}^{-2} \text{ s}^{-1}$ , rising to 1.0 (15 PSU) and then  
 386 dropping to 0.08 (30 PSU), reflecting the response of both  $W_{s(\text{Min})}$  and  $SPMC_{(\text{Min})}$  to changes in  
 387 salinity.

388 The EPS floc data show some interesting differences in behaviour to the equivalent mineral  
 389 tests. Contrary to that observed for mineral SPM, floc size ( $D_{(\text{Bio})}$ ) clearly decreases in a step-  
 390 wise manner under  $\tau_{Hi}$  conditions as salinity increases (Figure 3), where as the mean settling  
 391 velocity ( $W_{s(\text{Bio})}$ ) increases as salinity increases from 0 – 15 PSU, but then decreases at 30 PSU.

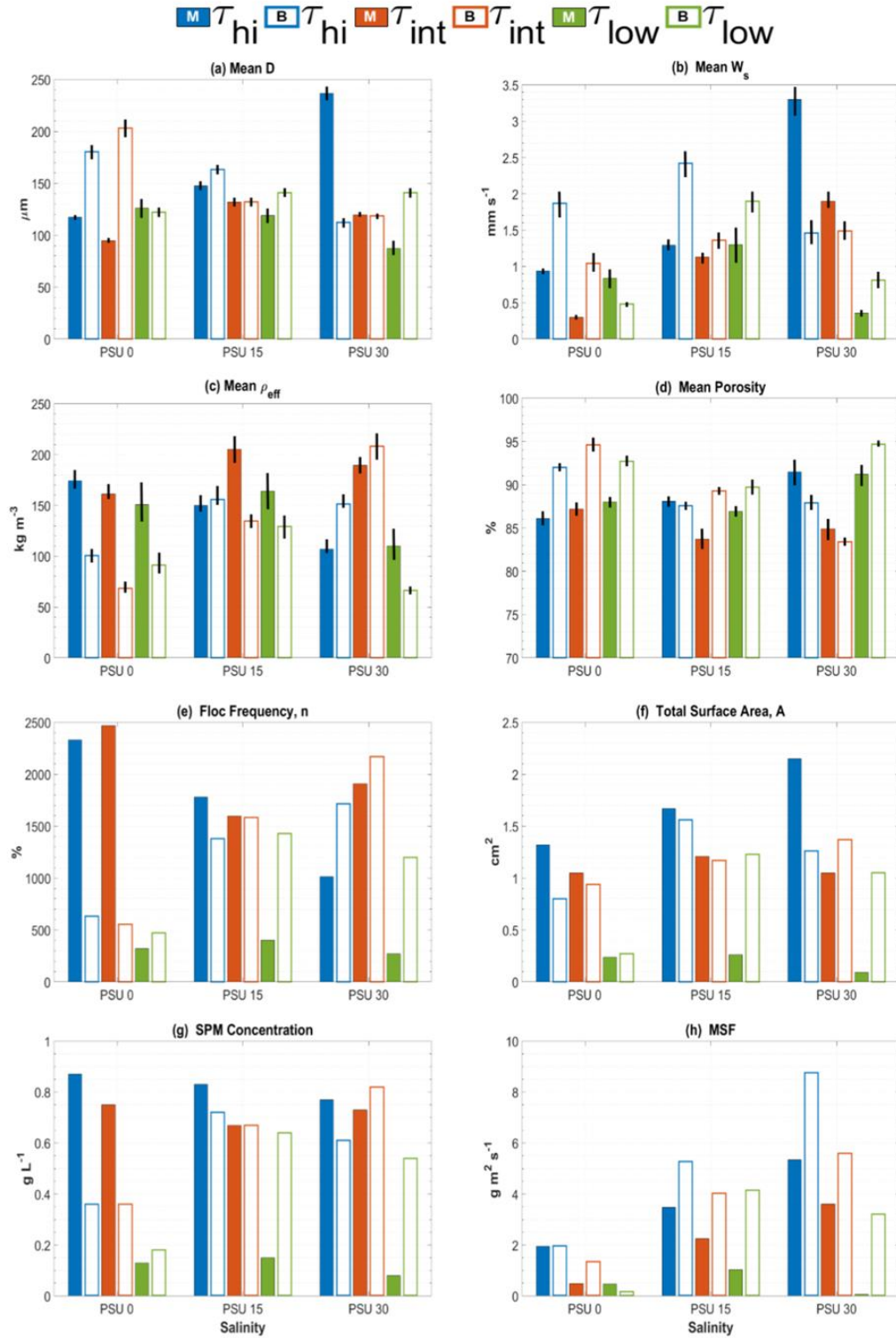


**Figure 3: Primary floc characteristics for the varying salinity and turbulence. Error bars in (a) – (d) are confidence intervals at 95%. Solid bars indicate results for mineral SPM; bars with colour outlines indicate results for biotic SPM.**

Changes in floc density ( $\rho_{eff(Bio)}$ ) are commensurate with those for  $W_{s(Bio)}$  driven by changes in porosity ( $Por_{(Bio)}$ ) which shows an inverse relationship to  $W_{s(Bio)}$  and  $\rho_{eff(Bio)}$ .  $SPMC_{(Bio)}$  increases from 0 to 15 PSU, then drops again at 30 PSU, reflecting changes in the mean density of the flocs, which dominates over the decrease in floc size ( $D_{(Bio)}$ ) and increase in floc frequency ( $n_{(Bio)}$ ).  $MSF_{(Bio)}$  under  $\tau_{Hi}$  conditions increases significantly with salinity by a factor of 4.5. It is clear that the higher  $MSF$  for the biotic SPM is driven by a lower settling velocity and higher effective density compared with mineral-only flocs (Figure 3).

Under  $\tau_{Int}$  conditions,  $D_{(Bio)}$  decreases with salinity as seen for the high turbulence tests (Figure 3). This is contrary to the rise and fall of  $D_{(Min)}$  under  $\tau_{Int}$ . Notably,  $D_{(Bio)}$  is the largest mean floc size across all of the EPS experiments. Mean settling velocities ( $W_{s(Bio)}$ ) rise from 0 to 30 PSU, with values around half those seen for  $\tau_{Hi}$ , as does the floc density ( $\rho_{eff(Bio)}$ ) (Figure 3). Compared with  $W_{s(Min)}$  under  $\tau_{Int}$  conditions,  $W_{s(Bio)}$  is higher for 0 and 15 PSU, but lower at 30 PSU, which is the opposite to the behaviour of the floc density. At the intermediate turbulence, the total surface area of the floc ( $A_{(Bio)}$ ) increased steadily with salinity consistent with the floc frequency and  $SPMC_{(Bio)}$ . Given the reduction in  $D_{(Bio)}$  it can be concluded that initially the SPM is comprised of large flocs which disaggregate into smaller flocs as salinity increases, yielding an increase in total surface area.  $SPMC_{(Bio)}$  is maintained at a relatively high concentration because of floc density differences ( $\rho_{eff(Bio)} < \rho_{eff(Min)}$ ).  $MSF_{(Bio)}$  values increase with salinity under intermediate shear conditions in a similar manner seen for  $\tau_{Hi}$ , resulting from increases in  $W_{s(Bio)}$  and  $SPMC_{(Bio)}$  which negate reductions in  $\rho_{eff(Bio)}$  (Figure 3). However,  $\tau_{Int}$  values are significantly lower than  $\tau_{Hi}$  for all salinities. Conversely, biotic SPM yields higher  $MSF_{(Bio)}$  values than  $MSF_{(Min)}$  under  $\tau_{Int}$  from freshwater to full salinity.

Under the lowest turbulence conditions the floc size ( $D_{(Bio)}$ ) only exhibits a small increase with salinity compared with a reduction in size for  $D_{(Min)}$ . Mean settling velocity ( $W_{s(Bio)}$ ) and floc density ( $\rho_{eff(Min)}$ ) both rise between 0 and 15 PSU, but then decrease at 30 PSU. Floc frequency

( $n$ ), surface area  $A_{(Bio)}$  and  $SPMC_{(Bio)}$  all show the same trend of an increase from 0 to 15 PSU then a slight decrease at 30 PSU (as was the case for the mineral tests) but in all cases the overall magnitudes of the values were significantly higher in the case of the EPS tests. However, the mass settling flux ( $MSF_{(bio)}$ ) at 0 PSU was significantly lower than the equivalent mineral value, but under saline conditions  $MSF_{(Bio)}$  was greater for the low turbulence tests.

Overall, for mineral SPM, an increase in salinity promotes floc growth at  $\tau_{Hi}$ , reflecting the electrostatic charging of the sediment.  $D_{(Min)}$  is positively related to salinity and doubles from freshwater to seawater salinity. The full seawater flocs under  $\tau_{Hi}$  exhibit settling velocities ( $W_{s(Min)}$ ) and effective floc density ( $\rho_{eff(Min)}$ ) more than 3-times slower and were nearly twice as dense. Conversely, there is a reduction in  $D_{(Bio)}$  and a commensurate increase in  $n$  under  $\tau_{Hi}$  and  $\tau_{Int}$  conditions as salinity increases. This indicates that salinity acts to reduce the influence of EPS in binding particles. Notably, the largest mean floc size across all experiments is for biotic SPM in freshwater. This indicates that flocculation efficiency is enhanced by the presence of EPS in freshwater (Zhoa et al., 2011), generating larger, more porous flocs with lower densities (Klimpel and Hogg, 1999). However, in saline conditions differences in porosity between mineral and biotic SPM varies and is dependent on the shear stress ( $\tau$ ). This is obviously a key variable within the estuarine environment where owing to tidal fluctuations (ebb and flow, neap and spring), varying river water flows and estuarine topography and bathymetry the shear stress is highly variable throughout its length (Manning, 2004).

$D_{(Min)}$  drops with  $\tau$  for saline conditions. This is because collisions facilitating floc formation from primary particles are less numerous in lower turbulence. Conversely, mean floc size and frequency and  $SPMC$  are notably higher for biotic SPM under  $\tau_{Low}$  saline conditions, despite higher settling velocities, indicative of the capacity of EPS to maintain flocs as turbulent mixing decreases. Total surface area is an important consideration with respect to the availability of sorption sites of the suspended sediment. It is a function of floc size and frequency. The total



surface area of mineral SPM is principally controlled by changes in floc size for  $\tau_{Hi}$  and  $\tau_{Int}$  conditions, but under  $\tau_{Low}$  conditions  $n_{(Min)}$  dictates  $A_{(Min)}$ .  $A_{(Bio)}$  is principally a function in  $n_{(Bio)}$  with the exception of  $\tau_{Hi}$  conditions across 15-30 PSU.

Mass settling flux increases with salinity for both mineral and biotic SPM, and both exhibit a stepwise reduction across turbulent regimes for each salinity. Under saline conditions  $MSF_{(Bio)}$  is substantially higher than  $MSF_{(Min)}$ , most notably under the lowest turbulent shear stress due to the high residency time of flocs containing EPS. Typically, larger flocs have faster settling velocities, but have a lower density and are therefore more porous. Consequently although the SPM concentration and density are lower, mass settling fluxes can increase because the settling rate outweighs the reductions in SPMC. Overall it can be evidenced in this study that the presence of EPS leads to more complex sediment dynamics compared with a pure mineral system (Lai et al., 2018).

### 3.3 *Settling Flux of Particulate PTMs*

The data from this study allows, for the first time, the sediment flocculation characteristics to be combined with the observed sorption characteristics to explore the impacts of the flocculation process on the partitioning of the PTMs. Consequently, it is possible to derive the settling flux of the particulate PTM fraction for each PTM under each experimental scenario:

$$PSF = C_d \times MSF \quad [Eq. 3]$$

where  $MSF$  = mass settling flux ( $g\ m^{-1}s^{-1}$ ) and  $C_d$  = mass of PTM on particulates ( $mg\ kg^{-1}$ ).

Particulate settling fluxes ( $PSF$ ) for each PTM in each experimental run are shown in Figure 4 and Table S5. A comparison across each turbulent shear stress reveals that deposition rates for all PTMs are greatest (for biotic and mineral) under the highest turbulence ( $\tau_{Hi}$ ) conditions.

*PSF*, however, varies between PTMs with salinity. For As *PSF* increases moving from 0 to 15 PSU then then is similar or even decreases from 15 to 30 PSU, with  $PSF_{(bio)}$  being significantly greater than the mineral equivalent. For Cd, there was a reduction in both *PSF* for both biotic and mineral with increases in salinity, again with rates greatest under biotic conditions. Copper showed a generally increasing trend with salinity, although at low shear strength the *PSF* did decrease for both  $PSF_{(bio)}$  and  $PSF_{(min)}$ . For Ni and Zn comparison between the biotic and mineral tests were not consistent. *PSF* decreased consistently with salinity for the mineral experiments (particularly for Ni) but for the biotic conditions with EPS added, rates were highest for the 30 PSU conditions and were generally higher for the biotic tests compared with equivalent mineral ones. At 30 PSU the *PSF* showed a significant downward trend from high to low shear stress, which was not obvious for the mineral equivalent tests, although this may have been a result of *PSF* values being very low for Ni and Zn in these experiments making trends hard to discern. Lead exhibited increasing *PSF* with salinity for the biotic tests, with a trend of the *PSF* being highest for high turbulence and lowest for lowest shear stresses. For the mineral tests under high turbulence, Pb *PSF* changed little with salinity, but at intermediate and low turbulence *PSF* tended to increase between 0 and 15 PSU then decrease slightly at the highest PSU, with the rates at the intermediate turbulence being commensurately higher than the low shear stress conditions.

Table S6 shows *PSF* values for each PTM ranked by magnitude for SPM type, salinity and turbulent shear stress. Across all experimental runs and for biotic SPM the order of magnitude of *PSF* is Pb>Zn>Cu>As>Ni>Cd. For mineral SPM, the same order holds except that Cu>Zn. Comparison of highest and lowest values shows Pb is deposited at 45, 38 and 49 times the rate of Cd for all, mineral and biotic SPM, respectively.

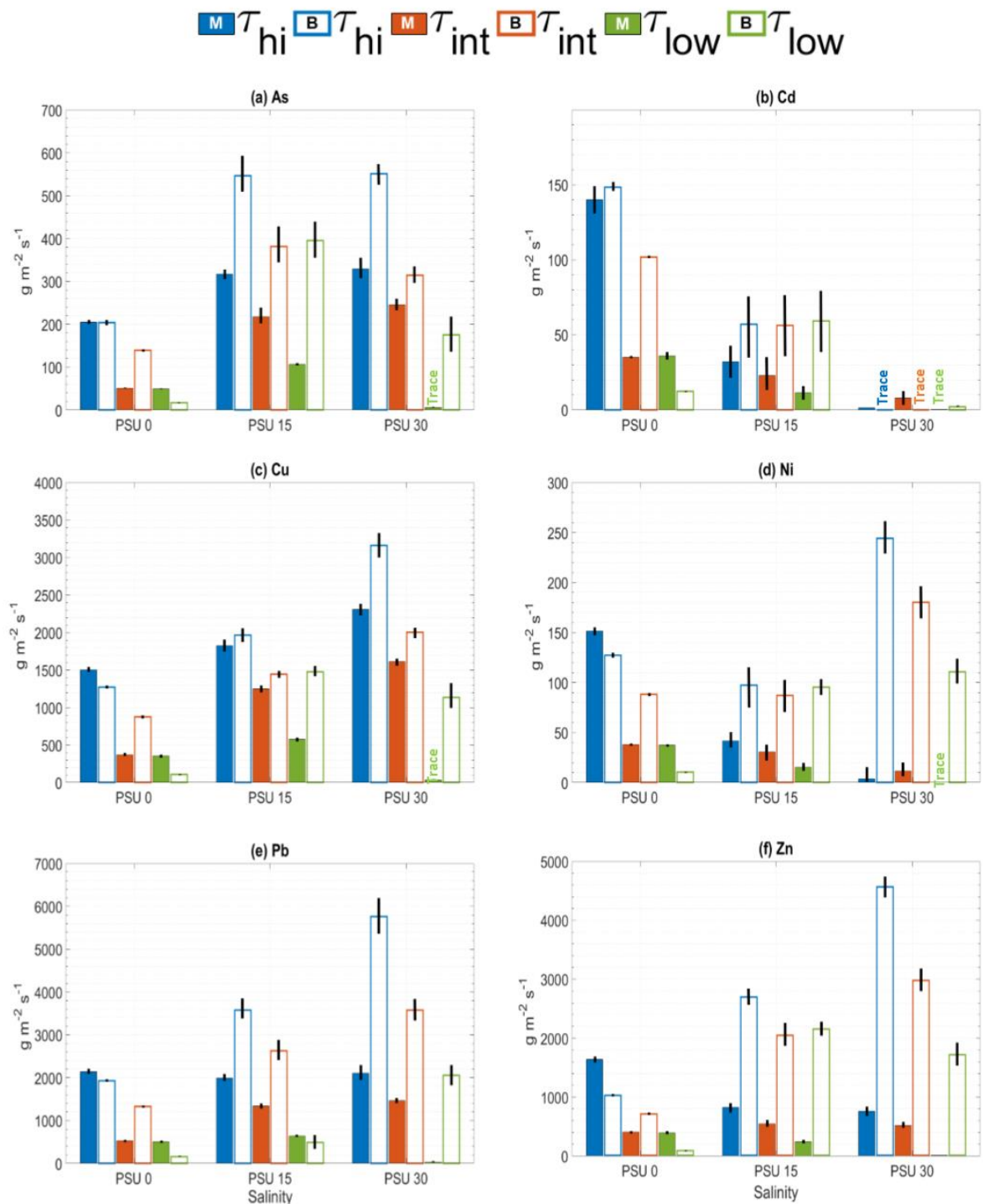


**Figure 4: Settling flux of particulate PTM,  $PSF$ , for each PTM for each experimental run. Solid bars indicate results for mineral SPM; bars with colour outlines indicate results for biotic SPM. Error bars are confidence intervals at 95%.**

Table S6b shows that particulate Pb is consistently deposited at the highest rate for each salinity. Cadmium exhibits the lowest rate of deposition for saline conditions, Ni for freshwater. Comparison of highest and lowest values shows that Pb is deposited 14 times faster than Ni in freshwater, 45 times faster than Cd in estuarine salinity and 1,362 times faster for ocean salinity.

#### **4. CONCLUSION**

Estuaries act as a critical conduit for the transfer of terrestrially-derived metal pollutants to coastal waters. By simulating the typical range of shear stresses, salinities and EPS contents within a cohesive estuarine environment this study has generated a dataset with which modellers and estuarine chemists can begin to untangle the complex interactions between the bio-physico-chemical processes controlling the fate of PTMs.

The data presented in this study has highlighted that the dynamic nature of an estuarine environment that leads to a constantly varying sorption dynamic between the main bio-physico-chemical parameters. This study reveals that salinity has the most significant role in dictating the particulate-phase settling flux of a range of common metal pollutants; the presence of EPS has a moderate effect; and changes to turbulent shear stress cause the least variation.

While the effects of chloro-complexation are well-known, the role of EPS is less understood.

Other studies have reported the importance of dissolved organic matter in controlling the partitioning of metals in contaminated estuaries via organic colloidal matter stabilising metals in the dissolved phase (Wang et al., 2017). As has been shown in this study, there is a complex interplay between the PTMs, complexation by dissolved organic matter and the role organic compounds, particularly EPS, play in both complexation but also the particle flocculation process. The results show that the presence of EPS considerably modifies sorption dynamics. Under freshwater conditions it reduces  $K_p$  for all PTMs compared with

mineral-only conditions. Conversely, in most cases under saline conditions  $K_p$  is greater when EPS is present.

Results highlight the importance of considering cohesive sediments in understanding the fate of PTMs. Flocs are porous and therefore offer a greater area for PTM sorption. Changes in floc size and suspended particulate matter concentrations also influence the sorption characteristics of the flocculating particles. Flocculation efficiency is enhanced by the presence of EPS in freshwater (see also Zhou et al., 2011), generating larger, more porous flocs with lower densities. While salinity acts to reduce the influence of EPS in binding particles compared to freshwater, total surface area is larger than biotic conditions due to greater floc frequency and lower settling rates, which maintains flocs in suspension.

Consequently, EPS increases the rate at which sediment settles under saline conditions, driven by a lower settling velocity and higher effective density compared with mineral-only flocs.

Parameters such as effective floc density and settling velocities have been shown in this study to span several orders of magnitude which has commensurate impacts on the partitioning of the PTMs between the dissolved and particulate phases. Moreover, an accurate representation of particulate-phase metal settling flux in cohesive sediments can only be achieved by characterizing the temporal and spatial variations in the mass settling flux of the flocculated suspended sediment. The deposition rates calculated here reflect the partition coefficients of the individual PTMs, which has been well reported for the natural estuarine environment (Comber et al., 1995; Turner et al., 2002), however the value of combining the partitioning characteristics of the PTMs with the sediment flocculation dynamics allows the estimation of flux of metals accumulating within sediments over time. The combination of changing partitioning coefficients and settling flux of the sediment yields several orders of magnitude difference in the deposition rate of metals bound to the sediment. The settling rate of particle-bound metals tends to be greatest for biotic rather than mineral-only sediments in saline

water. The pattern is reversed in freshwater largely due to lower  $K_p$  values resulting from the presence of EPS.

Incorporation of the metals into organic-rich particulate matter may also act as a way of stabilising the metal in the sedimentary phase, contributing to the diagenesis of the PTMs and removal from any further biological processing (Jokinen et al., 2020). With a knowledge of turbulence associated with an estuarine environment, with these deposition rate calculations it would be possible to determine areas of sediment and therefore metal accumulation and therefore identify parts of estuaries most likely to be at risk of levels building up to be a risk to benthic flora and fauna or are being sequestered, thus decreasing their risk.

There is a growing interest and concern regarding the influence sediment bound PTMs on in situ organisms and its interaction with overlying waters (Environment Agency, 2018). The data presented in this study highlights the need to consider a holistic approach to determining the fate of PTMs, from above the tidal limit to the coastal zone, taking account of the highly dynamic spatial and temporal nature of these environments. Although flocculation is secondary to salinity in terms of partitioning, it plays a critical role in sediment deposition and therefore PTM accumulation in bed sediments, with EPS significantly impacting on the partitioning and flocculation processes. Undertaking any risk assessment or modelling not taking account of the impacts of EPS on the partitioning of PTMs within a dynamic sediment environment are likely to lead to a bias in any outcomes or predictions.

Measurement of metals and flocculated sediments is resource intensive and logistically difficult, not least in developing countries or remote locations. Consequently, numerical modelling plays an important role in understanding the fate of dispersed metals. This study offers a framework in which to develop improved numerical modelling parameterisations of both soluble and particulate-phase PTMs. The provision of partitioning coefficients that represent the response of each metal to biological, physical and chemical variations provide a

basis for a dynamic partitioning coefficient. When implemented within combined flow & sediment models, particularly those that consider flocculation, relative proportions of soluble and particulate-phase metal content can be subject to appropriate flow and sediment transport calculations. Such an approach facilitates the management of environmental threats in the short-term, e.g., an at-a-point accidental release of PTMs, or in the long-term, e.g., the accumulation of PTMs in different spatial locations within a catchment.

### **Acknowledgements:**

The authors would like to thank Dr's Andy Fisher and Rob Clough for assistance in the analytical aspects of this work. The work was funded by Plymouth University's Seale Hayne Educational Trust and Marine Institute.

### **Conflict of Interest Statement**

The authors can confirm that there are no conflicts of interest associated with this work.

### **References**

- Benoit G., Oktay-Marshall S.D., Cantu II A., Hood E.M., Coleman C.H., Corapcioglu M.O., Santschi P.H., Partitioning of Cu, Pb, Ag, Zn, Fe, Al, and Mn between filter retained particles, colloids, and solution in six Texas estuaries, *Marine Chemistry*, 45, pp 307-336, 1994.
- Gerbersdorf, S. U., Westrich, B., Paterson, D. M. Microbial extracellular polymeric substances (EPS) in fresh water sediments. *Microb. Ecol.* 58, 334–349, 2009.
- Black, K. S., T. J. Tolhurst, T.J., Paterson, D. M., Hagerthey, S. E., Working with natural cohesive sediments, *Journal of Hydraulic Engineering*, 128, 2–8, 2002.
- Comber, S.D.W., Gardner M.J., Gunn A.M., Whalley C., Kinetics of trace metal sorption to estuarine suspended particulate matter. *Chemosphere*, 33, 1027-1040, 1996.

593 Comber, S.D.W., Gunn A.M., Whalley, C., Comparison of the partitioning of trace metals in  
 594 the Humber and Mersey estuaries. *Marine Pollution Bulletin*, 30, 851-860, 1995.

595 Defonseca E.M., Neto J.A., McAlister J., Smith B., Fernandez M.A. and Baliero F.C. The role  
 596 of the humic substances in the fractioning of heavy metals in Rodrigo de Freitas Lagoon, Rio  
 597 De Janeiro, Brazil. *Annals of the Brazilian Academy of Sciences*, 85, 1289-1301, 2013.

598 DEFRA, Water Framework Directive implementation in England and Wales: new and updated  
 599 standards to protect the water environment, UK, 44 pp, 2014.

600 Dennis, I.A., Macklin, M.G., Coulthard, T.J., Brewer, P.A., The impact of the October–  
 601 November 2000 floods on contaminant metal dispersal in the River Swale catchment, North  
 602 Yorkshire, UK, *Hydrological Processes*, 17, 1641-1657, 2003.

603 Dyer, K., Manning, A.J., Observation of the size, settling velocity and effective density of flocs,  
 604 and their fractal dimensions. *Journal of Sea Research*, 41, pp 87-95, 1998.

605 Elliott, M. and McLusky, D.S., The need for definitions in understanding estuaries. *Estuarine,*  
 606 *Coastal and Shelf Science*, 55, 815-827, 2002.

607 Environment Agency, Water Framework Directive, Update, 131 pp, 2011.

608 Environment Agency. SeDiChem Technical Report, Impact of sediment disturbance on  
 609 chemical status. Report no. EcoSF2/18/269, 2018.

610 Feng C., Guo X., Tian C. and Li Y. Heavy metal partitioning of suspended sediment matter-  
 611 water and sediment-water in the Yangtze estuary. *Chemosphere*, 185, 717-725, 2017.

612 Hanlon A.R.M., Bellinger B., Haynes K., Xiao G., Hofmann T.A., Gretz M.R., Ball A.S.,  
 613 Osborn A.M., Underwood G.J.C. Dynamics of extracellular polymeric substance (EPS)  
 614 production and loss in an estuarine, diatom-dominated, microalgal biofilm over a tidal  
 615 emersion–immersion period. *Limnol. Oceanogr.*, 1, 79-93, 2006.



616 Healy, T., Wang, Y., Healy, J.A., Muddy Coasts of the World: Processes, Deposits and  
 617 Function: Amsterdam, Elsevier, 556 pp, 2002.

618 Heiro A., Olias M., Canovas C.R., Martin J.E. and Bolivar J.P. Trace metal partitioning over a  
 619 tidal cycle in an estuary affected by acid mine drainage (Tinto estuary, SW Spain). *Sci. of the*  
 620 *Tot. Environ.*, 497-498, 18-28, 2014.

621 Hong S., Candelone J.P., Patterson C.C., Boutron C.F., History of ancient copper smelting  
 622 pollution during roman and medieval times recorded in green land ice, *Science*, 1669;  
 623 272(5259), pp 246–249, 2018.

624 Howarth R. W., J. R. Fruci J.R., Sherman D., Input of sediment and carbon to an estuarine  
 625 ecosystem: Influence of land use. *Ecological Applications*, 1, pp 27–39, 1991.

626 Hudson-Edwards, K.A., Macklin, M.G., Taylor, M.P. 2000 years of sediment-borne heavy  
 627 metal storage in the Yorkshire Ouse basin, NE England, UK, *Hydrological Processes*, 13,  
 628 1087-1102, 1999.

629 Jokinen S.A., Jilbert T., Filppula R.T. and Koho K., Terrestrial organic matter input drives  
 630 sedimentary trace metal sequestration in a human impacted boreal estuary. *Sci. of the Tot.*  
 631 *Environ.*, 717, 137047, 2020.

632 Kiørboe, T., Formation and fate of marine snow: small-scale processes with large- scale  
 633 implications, *Scientia Marina*, 65, 57-71, 2001.

634 Klimpel R.C., Hogg R., Effects of flocculation conditions on agglomerate structure. *Journal of*  
 635 *Colloid Interface Science*, 113, pp 121-131, 1986.

636 Koron, N., Faganeli, J., Falnoga, I., Mazej, D., Klun, K., Kovac, N., Association of  
 637 macroaggregates and metals in coastal waters, *Marine Chemistry*, 157, pp 185-193, 2013.

638 Lai H., Fang, H., Huang, L., He, G., Reible, D. A review on sediment bioflocculation:  
639 Dynamics, influencing factors and modelling, *Science of the Total Environment*, 642, 1184-  
640 1200, 2018.

641 Luoma S.N., Rainbow P.S., Metal contamination in aquatic environments. Science and lateral  
642 management, New York, U.S.A., 573 pp, 2008.

643 Machado, A.A.S., Spencer, K., Kloas, W., Toffolon, C.Z., Metal fate and effects in estuaries:  
644 A review and conceptual model for better understanding of toxicity, *Science of the Total*  
645 *Environment*, 541, 268-281, 2016.

646 Malarkey, J., Baas, J.H., Hope, J.A., Aspden, R.J., Parsons, D.R., Peakall, J., Paterson, D.M.,  
647 Schindler, R.J., Ye, L., Lichtman, I.D., Bass, S.J., Davies, A.G., Manning, A.J., & Thorne,  
648 P.D. The pervasive role of biological cohesion in bedform development, *Nature*  
649 *Communications*, 6, 6257-6261, 2015.

650 Manning A.J., Dyer K.R., A laboratory examination of flocc characteristics with regard to  
651 turbulent shearing, *Marine Geology*, 160, 147-170, 1999.

652 Manning A.J., Whitehouse R.J.S., Plymouth University Mini-annular flume – operation and  
653 hydrodynamic calibration. HR Wallingford Technical Report TR 169, UK, 2009.

654 Manning A.J., Observations of the properties of flocculated cohesive sediment in three Western  
655 European estuaries. *Journal of Coastal Research Special Issue*, SI 41, pp 70–81, 2004.

656 Manning, A.J., Whitehouse, R.J.S., Uncles, R.J. Suspended particulate matter: the  
657 measurements of flocs. In: R.J. Uncles and S. Mitchell (Eds), *ECSA practical handbooks on*  
658 *survey and analysis methods: Estuarine and coastal hydrography and sedimentology*, pp. 211-  
659 260, Pub. Cambridge University Press, 2017.

660 Matta J., Milad M., Manger R., Tosteson T., Heavy metals, lipid peroxidation, and  
 661 cigateratoxicity in the liver of the Caribben barracuda (*Sphyaena barracuda*), Biological Trace  
 662 Element Research, 70 , pp. 69-79, 1999.

663 Meadows, P.S., Meadows, A., Murray, J.M.H., Biological modifiers of marine benthic  
 664 seascapes: Their role as ecosystem engineers, Geomorphology, 157–158, 31–48, 2012.

665 Millennium Ecosystem Assessment: Ecosystems and Human Well-Being, (Eds.) Sarukhan, J.,  
 666 Whyte, A., Hassan, R., Scholes, R., Island Press, Washington, DC, 2005.

667 Miller J.R, Lechler P.J, Mackin G., Germanoski D., Villarroel L.F., Evaluation of particle  
 668 dispersal from mining and milling operations using lead isotopic fingerprinting techniques, Rio  
 669 Pilcomayo Basin, Bolivia, Science of The Total Environment, 384, pp 355-373, 2007.

670 McCave I.N., Size spectra and aggregation of suspended particles in the deep ocean, Deep-Sea  
 671 Research, 31, pp 329-352, 1984.

672 Morelle J., Schapira M. and Claquin P. Dynamics of phytoplankton productivity and  
 673 exopolysaccharides (EPS and TEP) pools in the Seine Estuary (France, Normandy) over  
 674 tidal cycles and over two contrasting seasons. Mar. Environ. Res., 131, 162-176, 2017.

675 Motekaitis R.J. and Martell A.E., Speciation of metals in the oceans. i. Inorganic complexes in  
 676 seawater, and influence of added chelating agents. Marine Chemistry, 21, 101-116, 1987.

677 Nho N.T., Strady E., Trang T., David F. and Marchand C. Trace metals partitioning between  
 678 particulate and dissolved phases along a tropical mangrove estuary (Can Gio, Vietnam).  
 679 Chemosphere, 196, 311-322, 2018.

680 Parsons, D. ,R., Schindler, R.J., Hope, J.A., Malarkey, J., Baas, J.H., Peakall, J., Manning,  
 681 A.J., Ye, L., Simmons, S., Paterson, D.M., Aspden, R.J., Bass, S.J., Davies, A.G., Lichtman,  
 682 I.D., Thorne, P.D., The role of bio-physical cohesion on subaqueous bedform size, Geophysical  
 683 Research Letters, 43, 1566–1573, 2016.

684 Paterson, D.M., Yallop, M.L., Wellsbury, P., Inter-relationships between rates of microbial  
685 production, exopolymer production, microbial biomass and sediment stability in biofilms of  
686 intertidal sediments, *Microbial Ecology*, 39, 116-127, 2000.

687 Singh K.P., Malik A., Sinha S., Estimation of Source of Heavy Metal Contamination in  
688 Sediments of Gomti River (India) using Principal Component Analysis. *Water Air & Soil*  
689 *Pollution*, 166, 321–341, 2005.

690 SKB, Solid/liquid partition coefficients (K<sub>d</sub>) for selected soils and sediments at Forsmark and  
691 Laxemar-Simpevarp, Denmark, 102 pp, 2009.

692 Spears B.M., Saunders J.E., Davidson I., Paterson D.M. Microalgal sediment biostabilisation  
693 along a salinity gradient in the Eden Estuary, Scotland: unravelling a paradox. *Marine and*  
694 *freshwater Research*, 59, 313-321, 2007.

695 Spencer, K.L., MacLeod, C.L., Tuckett, A., Johnson, S.M., Source and distribution of trace  
696 metals in the Medway and Swale estuaries, Kent, UK, *Marine pollution Bulletin*, 52, 214-238,  
697 2006.

698 Taylor M.P., Hudson-Edwards, K.A., The dispersal and storage of sediment-associated metals  
699 in an arid river system: The Leichhardt River, Mount Isa, Queensland, Australia,  
700 *Environmental Pollution*, 152, 193-204, 2008.

701 Turner A., Millward G.E., Suspended Particles: Their Role in Estuarine Biogeochemical  
702 Cycles, *Estuarine, Coastal and Shelf Science*, 55, 857-883, 2002.

703 Turner, A., Trace-metal partitioning in estuaries: importance of salinity and particle  
704 concentration. *Marine Chemistry*, 54, 27-39, 1996.

705 Turner A. Millward G.E., LeRoux S.M. Significance of oxides and particulate organic matter  
 706 in controlling trace metal partitioning in a contaminated estuary. *Mar. Chem.*, 88, 179-192,  
 707 2004.

708 Van der Auweraert E. (2018) Trace metal pollution in the Scheldt estuary – a statistical  
 709 approach to estimate metal partitioning coefficient for a suite of metals. PhD Thesis, Delft  
 710 University of Technology, Sept 30, 2018.

711 Wang W. and Wang W.X. Phase partitioning of trace metals in a contaminated estuary  
 712 influenced by industrial effluent discharge. *Environmental Pollution*, 214, 35-44, 2016.

713 Wang W., Chen M., Guo L. and Wang W.X. Size partitioning and mixing behaviour of trace  
 714 metals and dissolved organic matter in a south China Estuary. *Sci. of the Tot. Environ.*, 603-  
 715 604, 434-444, 2017.

716 Wells R., Impact of sediment disturbance on chemical status. Environment Agency report  
 717 SC180002, UK, 53 pp, 2019.

718 Zwolsman, J.J.G, Berger, G.W., Van Eck, G.T.M., Sediment accumulation rates, historical  
 719 input, post-depositional mobility and retention of major elements and trace metals in salt marsh  
 720 sediments of the Scheldt estuary, SW Netherlands, *Marine Chemistry*, 44, 73-94, 1993.